I&EC research
Industrial & Engineering Chemistry Research

ACS Editors' Choice

Article

pubs.acs.org/IECR

Use of Vanadium(V) Oxide as a Catalyst for CO_2 Hydration in Potassium Carbonate Systems

Nathan Johann Nicholas, Gabriel da Silva, Sandra Kentish, and Geoffrey W. Stevens*

The Cooperative Research Centre for Greenhouse Gas Technologies (CO2CRC), Department of Chemical and Biomolecular Engineering, The University of Melbourne, Parkville, Victoria 3010, Australia

Supporting Information

ABSTRACT: The kinetics of CO_2 absorption into 30% w/w K_2CO_3 solutions containing 0.1−0.5 M $K_4V_2O_7$ was investigated at temperatures of 40, 60, and 75 °C using a wetted wall column. Vanadium(V) speciation diagrams were developed under these conditions as a function of CO_2 loading using ^{51}V NMR spectroscopy. From these studies it was determined that there are two oxyvanadate ions that promote the absorption of CO_2, HVO_4^{2-}, and $HV_2O_7^{3-}$. The Arrhenius expressions for the rate constants of these two species were found to be $k_{HVO_4} = 2 \times 10^{11} \exp(-4992/T)$ and $k_{HV_2O_7} = 5 \times 10^{18} \exp(-10218/T)$, respectively. Comparison of the observed rate constants with other promoters revealed that both active vanadium species showed performances comparable with that of MEA and vastly superior performances over those of other inorganic promoters. Due to speciation changes as the vanadium concentration is increased, the relative performance of vanadium diminished with increasing total vanadium concentration. As such, vanadium may be more suitable as a secondary component and corrosion inhibitor in a promoted carbonate system.

INTRODUCTION

The release of greenhouse gases, particularly carbon dioxide (CO_2), into our atmosphere is becoming an increasing global concern. This is not only for the potential of increased atmospheric CO_2 levels to influence climate change,[1−3] but also to increase the acidification of our oceans.[4−7] In an effort to reduce these effects on our world, there is increasing research being undertaken to reduce CO_2 emissions by selectively removing it from the exhaust gas streams of industrial sources, particularly coal fired power stations.

Many different types of technologies are currently being developed to reduce CO_2 emissions.[8,9] Of these technologies solvent absorption is the most advanced, with CO_2 capture using aqueous amines (such as piperazine[10,11] or monoethanolamine[12,13] (MEA)) being the current industry benchmark for CO_2 capture technologies.[8,11]

While amine systems show great potential for CO_2 capture solvents, due to their high CO_2 absorption rates[11,13,14] and high CO_2 capacity,[15] they are not without their drawbacks. Besides their high toxicity and corrosivity,[16] amines often have high vapor pressures,[17] resulting in significant solvent losses and contaminated exit gas streams. Furthermore, amines are prone to oxidative and thermal degradation,[16,18−20] and can react with other gases often present in industrial CO_2 streams (namely NO_x and SO_x), forming inactive, thermally stable salts.[21]

A potential alternative solvent system to aqueous amines is the use of aqueous solutions of potassium carbonate (K_2CO_3). The Benfield process for absorbing CO_2 into potassium carbonate systems was first developed in the 1950s;[22−24] however, the system has undergone renewed interest in recent times as an alternative to amine based systems.[25,26]

In the carbonate system CO_2 is absorbed into the solution and converted to bicarbonate ions via the following reaction scheme:

$$CO_2(g) \rightleftharpoons CO_2(aq) \quad (1)$$

$$CO_2(aq) + H_2O(l) \rightleftharpoons H_2CO_3(aq) \quad (2)$$

$$H_2CO_3(aq) \rightleftharpoons H^+(aq) + HCO_3^-(aq) \quad (3)$$

$$CO_2(aq) + OH^-(aq) \rightleftharpoons HCO_3^-(aq) \quad (4)$$

$$H_2O(l) \rightleftharpoons OH^-(aq) + H^+(aq) \quad (5)$$

$$CO_3^{2-}(aq) + H^+(aq) \rightleftharpoons HCO_3^-(aq) \quad (6)$$

This gives the overall reaction (on the liquid side) as

$$CO_2(aq) + H_2O(l) + CO_3^{2-}(aq) \rightleftharpoons 2HCO_3^-(aq) \quad (7)$$

where the hydration of CO_2 (predominantly via eq 4) is the rate-determining step.

There are many advantages to using K_2CO_3, namely, low corrosivity, low volatility, high tolerance to gaseous impurities (i.e., SO_x, NO_x, and O_2), and high thermal stability. However, it does have one major disadvantage: a low rate of reaction with CO_2.[26,27] As a result, large process equipment utilizing large volumes of solvent is needed to reach the required level of CO_2 removal (~90%). This limitation can be overcome to some degree, however, by the introduction of a promoter into the solvent system. A promoter is a chemical species that accelerates the rate of CO_2 uptake by catalyzing the hydration of CO_2 into HCO_3^- or by rapidly chemically binding CO_2.

Of the different promoters available amine based compounds are presently the most viable as they are cheap to produce and

Received: November 21, 2013
Revised: January 29, 2014
Accepted: February 3, 2014
Published: February 3, 2014

   dx.doi.org/10.1021/ie403836e | Ind. Eng. Chem. Res. 2014, 53, 3029−3039

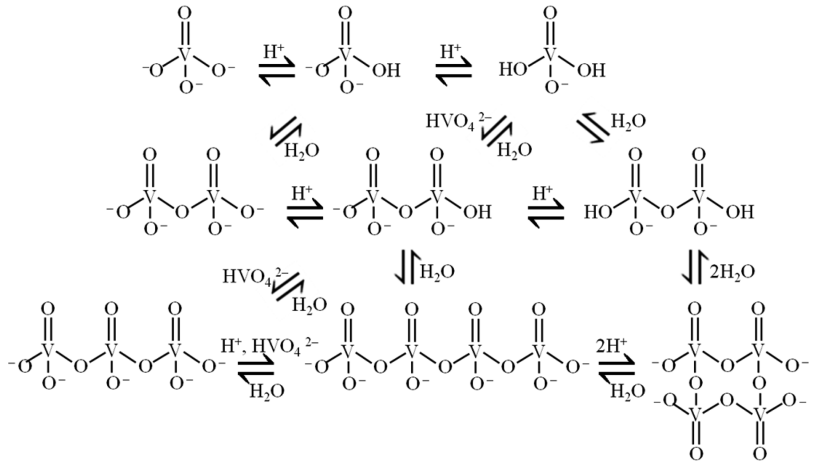

Figure 1. Simplified equilibrium diagram for vanadium(V) speciation in basic to pH neutral water. As pH decreases, the smaller anions become protonated and condense into larger anions.

offer exceptionally high rates of CO_2 absorption in carbonate solvents.[28,29] However, they often introduce some of the previously mentioned limitations that are present in pure and aqueous amine systems. Some of these limitations (such as high vapor pressure) can be overcome by using different classes of amines, such as amino acids.[30−32] However, they are still susceptible to oxidative and thermal degradation and can be corrosive.[16,33] Moreover, amines will react with CO_2 to form a stable carbamate that will only partially hydrolyze to yield HCO_3^-,[34] thus impacting upon the energy requirements of CO_2 regeneration. Aqueous inorganic ions, however, have the potential to overcome the shortcomings present in organic promoters. The presence of different inorganic ions, such as borate,[27,35] arsenite,[36−39] hypochlorite,[36,39] phosphate,[36] vanadate,[40] and silicate[36] has been shown to enhance the absorption of CO_2.

For an inorganic oxyanion to act as a catalyst for CO_2 hydration, it must possess certain properties. It cannot form a stable carbonate complex, it must have a pK_a in the range 8−11, and any negative charges must be localized.[36] Furthermore, if the anion has a labile hydroxyl group, its catalytic performance may be enhanced as this hydroxyl group can directly interact with the CO_2 via the carbonic anhydrase mechanism.[35,41] The carbonic anhydrase mechanism for CO_2 hydration involves the direct association of a CO_2 molecule with the OH group to form a bicarbonate complex. This complex is exchanged with a water molecule (releasing the bicarbonate ion), restoring the catalyst after a subsequent deprotonation step.

The work presented here is concerned with the performance of aqueous oxyanions of vanadium at catalyzing CO_2 hydration in concentrated (30% w/w) potassium carbonate solvents. Vanadium was chosen to be studied in this work, not only for its ability to enhance CO_2 absorption, but also for its ability to act as a corrosion inhibitor. However, it is difficult to interrogate the mechanism of vanadium(V) catalyzed CO_2 hydration in aqueous carbonate solutions because of the complex distribution of vanadium among a number of species. It has been well-established that aqueous solutions of vanadium(V) can form a wide variety of oxyanions, from monomers to decamers, each able to protonate to differing degrees.[42,43] This is due to a complex interplay of condensation reactions between the different ions and the acid/base equilibria of each ion, as illustrated in Figure 1. As the reaction constants of formation for the different vanadate species are similar, the speciation of vanadium is heavily dependent upon solution conditions, with pH, total concentration of vanadium, and temperature all influencing speciation. For instance, Figure 2 shows the speciation of vanadium as a function of pH (in 1.0 M $NaClO_4$ at 25 °C) at two total concentrations of vanadium: 0.1 and 0.5 M. At 0.1 M total vanadium concentration the principle species in the pH range 10−12 are HVO_4^{2-} (30−50%) and $V_2O_7^{4-}$ (20−50%), with the other species becoming

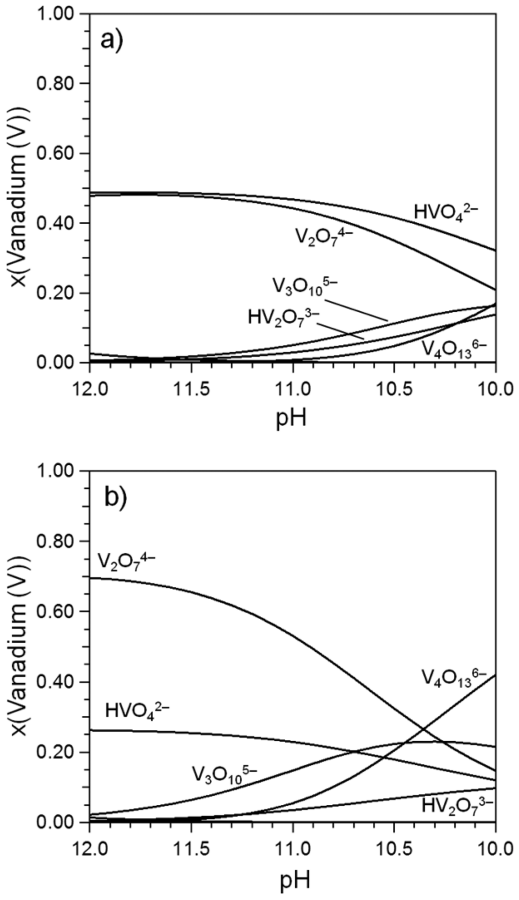

Figure 2. Speciation diagrams for (a) 0.1 and (b) 0.5 M vanadium(V) in 1.0 M $NaClO_4$ at 25 °C. Data generated using formation constants obtained from Cruywagen et al.[52]

dx.doi.org/10.1021/ie403836e | Ind. Eng. Chem. Res. 2014, 53, 3029−3039

significant only at the lower pH values. At 0.5 M vanadium the concentration of HVO_4^{2-} is significantly decreased (reduced to 10−25% of the total vanadium over the same pH range), while the $V_2O_7^{4-}$ becomes even more predominant in solution (15−70%), particularly at high pH values. Furthermore, the larger vanadate ions, $V_3O_{10}^{5-}$ and $V_4O_{13}^{6-}$, become more prevalent at lower pH values, comprising 20 and 40%, respectively, of the vanadium at pH 10.

It is also known that the presence of carbonate and bicarbonate ions heavily influences vanadium(V) speciation. Vermaire and De Haan[44] investigated the speciation of 0.04 M vanadium(V) in 0.25 M NaSCN as a function of different concentrations of carbonate (0.095−0.57 M) at a constant pH 8.5. They found that, as the concentration of carbonate (which at pH 8.5 is mainly present as the bicarbonate ion) increased, the concentration of the larger vanadium polyanions decreased, whereas the concentration of dimeric vanadate species increased. This indicates that the presence of carbonate encourages the formation of smaller vanadate ions at the expense of the larger ions.

This work aims to first characterize the speciation of vanadium(V) in basic aqueous carbonate solutions relevant to industrial carbon capture systems. Once a rigorous understanding of the relevant vanadium chemistry is established, we then consider the kinetics and mechanism of CO_2 hydration by vanadium(V) in carbonate solvents, identifying the active species and assigning temperature-dependent rate constant expressions to their reactions with CO_2. It should be noted that this work is only concerned with vanadium(V) complexes as these are most likely to be present in a solvent used for absorption of CO_2 from flue gases. It is possible that during solvent regeneration vanadium(IV) complexes could form and interact differently with CO_2, but these effects are beyond the scope of this paper.

MATERIALS AND METHODS

Materials. All chemicals used in this study were of analytical reagent grade and used without further purification. Potassium carbonate (99.8% Thasco Chemical Co. Ltd.) and potassium bicarbonate (≥99% Ajax Finechem Pty Ltd.) were used to prepare a 30% w/w K_2CO_3 solution with a known CO_2 loading. Vanadium(V) oxide (>99% Aldrich Chemistry) and potassium hydroxide (>90% Sigma Aldrich) were added to these solutions in a 1:4 (V_2O_5:KOH) molar ratio to create the desired concentration of potassium divanadate ($K_4V_2O_7$) in the potassium carbonate solution. Reverse osmosis water (resistivity 6.1 MΩ cm^{-1}) was used to make up the solutions. NMR standard samples were prepared using the above chemicals with D_2O (99.9% Cambridge Isotope Laboratories) instead of the usual reverse osmosis water. All solutions were left for at least 1 day to allow the vanadium speciation to come to equilibrium.

The 10.2% N_2−89.8% CO_2 gas mixture used in the wetted wall column studies was obtained from BOC Gases Australia Ltd.

Loading. Loading in this work is defined as moles of CO_2 absorbed per mole of carbonate present in an unloaded solution:

$$\text{loading} = \frac{n(CO_2)_{abs}}{n(K_2CO_3)_{unloaded}} \tag{8}$$

or

$$\text{loading} = \frac{[CO_2]_{tot} - [CO_2]_i}{[CO_2]_i} \tag{9}$$

where $[CO_2]_{tot}$ is the total concentration of CO_2 in the solution (i.e., the sum of the concentrations of carbonate, bicarbonate, and any vanadium carbonate complexes) and $[CO_2]_i$ is the concentration of CO_2 in an unloaded K_2CO_3 solution. As this work was performed in a 30% w/w carbonate solution, $[CO_2]_i$ is a constant value of 2.8 M.

Wetted Wall Column. Measurements of the kinetics of CO_2 absorption into aqueous K_2CO_3 containing different concentrations of $K_4V_2O_7$ were performed using a wetted wall column. In a wetted wall column (WWC) an inlet gas of known CO_2 concentration and flow rate is first passed through a water saturator at temperature, before being fed into the central chamber of the WWC. The central chamber of the WWC consists of a vertical open pipe of known dimensions centered in a larger cylindrical chamber. Liquid at a constant flow rate is pumped from a storage tank up the central pipe, where it overflows and cascades over the outer surface of the pipe in a thin laminar film of known thickness, before returning to storage tank. The saturated gas is fed via three evenly spaced vents at the base of the column, where it comes into contact with the laminarly flowing liquid stream in a countercurrent fashion, allowing mass transfer to occur over a controlled, well-defined area. The gas leaves at the top of the column and is passed through a subzero condenser, and the flow rate and CO_2 concentration of the dry gas stream are measured before venting. The central chamber is enclosed in a heated water jacket to maintain a constant temperature during the experiment. The characterization of the WWC has been previously published by our group.[27,29]

The conditions in the WWC were chosen such that the aqueous concentration of CO_2 was much lower than the concentrations of hydroxide and vanadate ions, and therefore pseudo-first-order kinetics could be assumed. Under these conditions the absorption rate (per unit area) of CO_2 can be expressed as[45]

$$N_{CO_2} = \frac{1}{\frac{1}{k_g} + \frac{H}{\sqrt{k_l^{\circ 2} + D_{CO_2} k_{obs}}}} (P_{CO_2} - P^*_{CO_2}) \tag{10}$$

where N_{CO_2} (mol m^{-2} s^{-1}) is the flux of CO_2 into the promoted potassium carbonate solution, k_g (mol Pa^{-1} m^{-2} s^{-1}) is the gas phase mass transfer coefficient, H (Pa m^3 mol^{-1}) is Henry's constant for CO_2 in carbonate solutions, k_l° (m s^{-1}) is the physical mass transfer coefficient in the liquid phase, D_{CO_2} (m^2 s^{-1}) is the diffusion coefficient of CO_2 in the solvent, and k_{obs} (s^{-1}) is the pseudo-first-order reaction rate constant (with respect to CO_2). The pseudo-first-order reaction rate constant can then be expressed as separate terms for each species that reacts with CO_2:

$$k_{obs} = k_i[i]^n + k_j[j]^m + \ldots \tag{11}$$

where k_i, k_j, etc. are the reaction rate constants for each active species, and n, m, etc. are the reaction orders with respect to each species.

As the concentrations of $K_4V_2O_7$ added to the potassium carbonate solutions were comparatively small, it was assumed they had negligible effect on the diffusivity and Henry's constant of CO_2, so previously reported values[46−50] for potassium carbonate solutions were used in this work.

dx.doi.org/10.1021/ie403836e | Ind. Eng. Chem. Res. 2014, 53, 3029−3039

NMR Spectroscopy. Speciation studies of $K_4V_2O_7$ in 30% w/w K_2CO_3 as a function of temperature, CO_2 loading, and total vanadium concentration were performed using an Agilent DD2 500 MHz NMR at 131.27 MHz, in the range −400 to −875 ppm using D_2O as an internal standard.

UV/Vis Spectrophotometry. The UV/vis spectra between 350 and 500 nm of 0.1−0.5 M $K_4V_2O_7$ in 30% w/w K_2CO_3 (0−0.35 loading) were obtained using a 5 mm path length polystyrene cuvette (Greiner Bio-One) with an unloaded 30% w/w K_2CO_3 solution used as a reference. As the samples could not be diluted (as dilution changed vanadium speciation), the wavelength at 75, 50, and 25% transmission was recorded as a function of loading and $K_4V_2O_7$ concentration.

RESULTS

Vanadium Speciation in Carbonate Solutions. From the observations stated previously it is expected that, as a vanadium containing carbonate solution absorbs CO_2, the vanadium speciation will change in a nonsimplistic manner. As the loading is increased the pH will decrease, encouraging the formation of the larger polyanions. However, the carbonate concentration will also increase, which should hinder the formation of large vanadate polyanions. With these competing influences it is difficult to predict the vanadium speciation behavior as a function of loading. As shown by eq 11, without knowledge of vanadium speciation the reaction rate constants of the different vanadium species cannot be determined. Therefore, the speciation of vanadium under the conditions where CO_2 absorption was studied must be determined. To accomplish this, ^{51}V NMR was used to examine the speciation present in a series of 24 standard solutions of different $K_4V_2O_7$ concentrations (0.1, 0.3, and 0.5 M) at various loadings (0−0.35 with 0.05 increments) at 25, 40, 60, and 75 °C.

Standard solutions were used (instead of the actual samples from the wetted wall experiments) because ^{51}V NMR required the presence of D_2O for an internal standard and it was not feasible to include the required amount of D_2O (a minimum of 10% by volume) in the large volume WWC experiments. Furthermore, the WWC samples could not be diluted with D_2O after the experiment as this would change the vanadium speciation.

An example of the ^{51}V NMR spectra obtained as a function of loading is given in Figure 3a. Each spectrum was deconvoluted into six distinct Gaussian peaks corresponding to different vanadates species as summarized in Table 1 and shown in Figure 3b.

These values were generally in good agreement with previously reported values for the different vanadate species.[42−44,51] The only exception was the peak at −567 to −573 ppm, which has previously been reported to be consistent with a $H_2V_2O_7^{2-}$ species.[42] However, the pK_a of this species is around 8.3,[42,52] and given the pH range of the solutions studied in this work was 10.3−11.5, there should be no appreciable amount of $H_2V_2O_7^{2-}$ present. Furthermore, as this peak was seen to increase with increasing bicarbonate and vanadium concentrations and it is known that acidic carbonates tend to react with vanadium oxyanions to form anhydride-like complexes,[53] the peak at −567 to −573 ppm is attributed to a vanadium carbonate complex (denoted as V-CO_2). The exact form of this vanadium carbonate complex is unknown, as a range of carbonate complexes are possible, and it was not possible to determine the exact form from the ^{51}V NMR spectra.

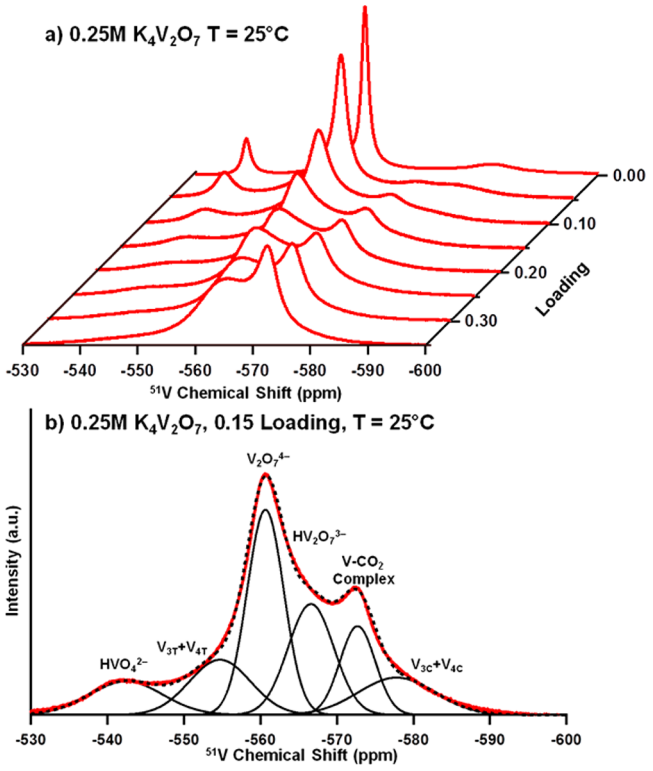

Figure 3. ^{51}V NMR spectra of 0.25 M $K_4V_2O_7$ in 30% w/w K_2CO_3 at (a) 0−0.35 CO_2 loading and (b) at 0.15 loading showing the peak location and contribution from each vanadium(V) species. As loading increases, the concentrations of HVO_4^{2-} and $V_2O_7^{4-}$ decrease, while the concentrations of $HV_2O_7^{3-}$ and the vanadium carbonate complex increase.

Using the area of each Gaussian peak to determine the relative amount of each species present, the concentration of each species as a function of temperature, vanadium concentration, and loading could be determined and can be found in the Supporting Information. The concentration of each species as a function of vanadium concentration and loading at 40 °C is given in Figure 4 as an example.

From Figure 4a it can be seen that the concentration of HVO_4^{2-} is relatively constant with increasing $K_4V_2O_7$ concentration, and it slightly decreases as the CO_2 loading increases. In contrast, the concentration of $V_2O_7^{4-}$ (Figure 4b) increases with increasing $K_4V_2O_7$ concentration but decreases with increased loading. Finally, the concentrations of $HV_2O_7^{3-}$ (Figure 4c), $V_3O_{10}^{5-}$, $V_4O_{13}^{6-}$ (Figure 4d), and the carbonate complex (Figure 4e) all increase with increasing $K_4V_2O_7$ concentration and (to a lesser extent) loading. These trends were observed to be consistent over all temperatures studied, though the absolute concentrations at a particular condition vary with temperature (see Supporting Information). It was also found that the thermal history of the sample did not affect the speciation as, at a given temperature, the speciation did not differ if the sample was heated to a higher temperature and then subsequently cooled, or simply heated to the desired temperature.

These results illustrate how the previously mentioned competing factors that influence vanadate speciation impact the different vanadate ions. For HVO_4^{2-} ions the decrease in pH associated with an increase in loading is mainly balanced by the increased concentration of bicarbonate ions; thus the $[HVO_4^{2-}]$ only increases slightly with loading. The $[V_2O_7^{4-}]$

dx.doi.org/10.1021/ie403836e | Ind. Eng. Chem. Res. 2014, 53, 3029−3039

Table 1. ^{51}V NMR Peak Location of Each Vanadate Species Observed in This Work[a]

	HVO_4^{2-}	$V_3O_{10C}^{5-}/V_4O_{13C}^{6-}$	$V_2O_7^{4-}$	$HV_2O_7^{3-}$	V-CO_2	$V_3O_{10T}^{5-}/V_4O_{13T}^{6-}$
peak shift range (ppm)	−539.0 to −546.0	−554.0 to −556.0	−559.0 to −561.5	−563.0 to −564.4	−567 to −573	−572 to −580

[a]C, central vanadate species; T, terminal vanadate species.

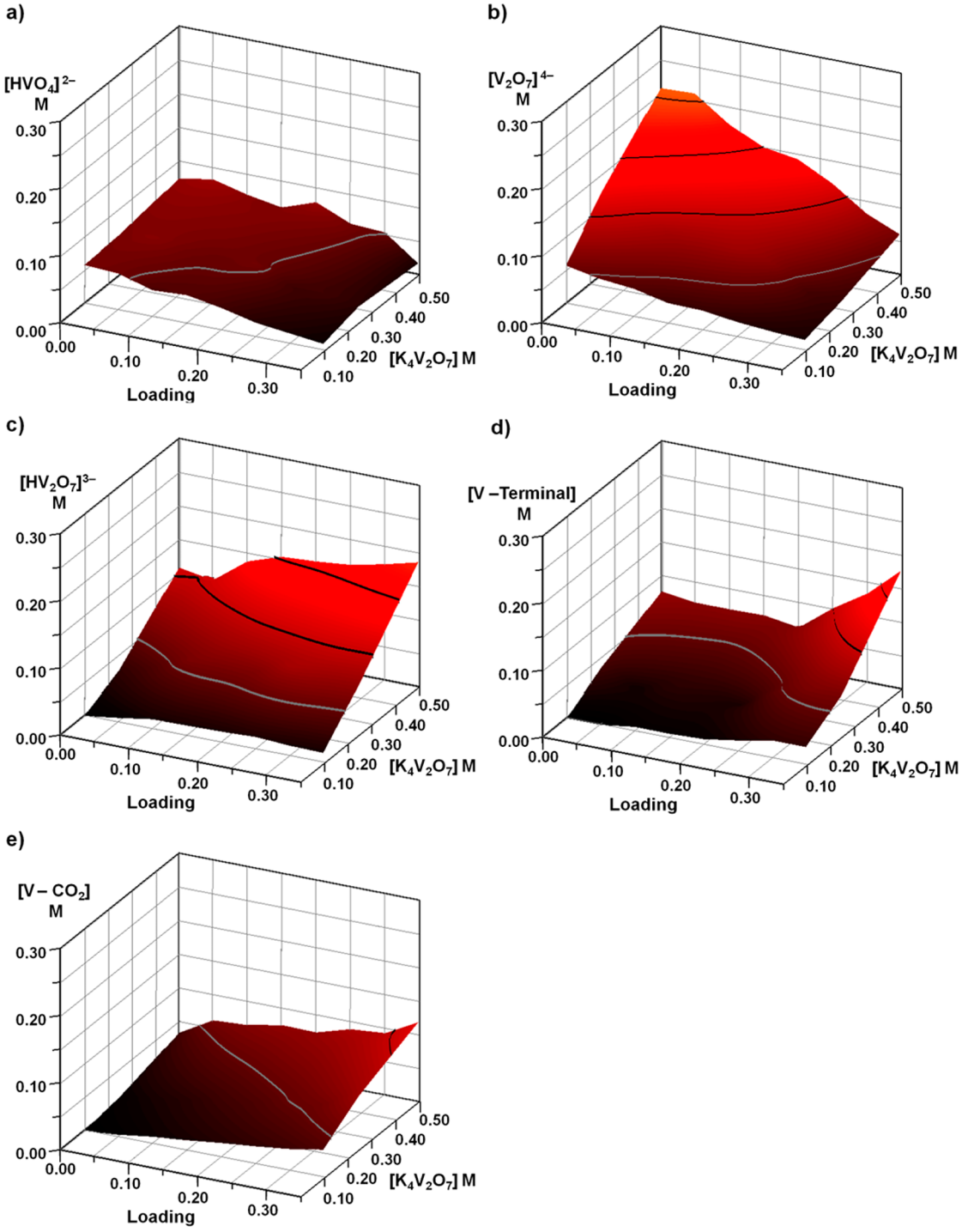

Figure 4. Concentration of (a) HVO_4^{2-}, (b) $V_2O_7^{4-}$, (c) $HV_2O_7^{3-}$, (d) terminal vanadates of $V_3O_{10}^{5-}/V_4O_{13}^{6-}$, and (e) vanadate carbonate complex as a function of $K_4V_2O_7$ concentration and CO_2 loading in 30% w/w K_2CO_3 at 40 °C. Contours indicate equal concentrations at 0.05 M intervals.

however is much more sensitive to the decrease in pH as it decreases significantly with an increase in loading. This effect becomes more pronounced as the total vanadium concentration increases. The formation of $HV_2O_7^{3-}$ ions is primarily dependent on the total vanadium concentration, with an increase in vanadium concentration encouraging the formation of these ions. The effects of loading are also dependent on total vanadium concentration. At higher vanadium concentrations

dx.doi.org/10.1021/ie403836e | Ind. Eng. Chem. Res. 2014, 53, 3029−3039

the decrease in pH dominates over the effects of bicarbonate, causing an increase in $[HV_2O_7^{3-}]$, whereas at lower vanadium concentrations the two effects balance each other, resulting in no concentration change with loading. The concentration of the larger polyvanadate ions only becomes significant at high loadings and high vanadium concentrations, where the solution is sufficiently acidic to overcome the destabilizing effects of the bicarbonate and there is a high enough concentration of vanadium to make the formation of polyvanadates favorable. Finally, the concentration of the vanadium carbonate complex is more sensitive to the increase in concentration of vanadium than the increase in bicarbonate ions, indicating that the concentration of reactive vanadate ions is the limiting factor in the carbonate complex formation.

To relate the samples obtained from the WWC experiments to the standard solutions, UV−vis spectroscopy was used, as the K_2CO_3 solutions containing vanadium turned from clear to green-yellow as the concentration of bicarbonate (and therefore loading) increased. The wavelength at which 25, 50, and 75% transmission occurred was recorded for solutions of known vanadium concentration and loading compared to the wavelengths of the samples obtained from the WWC experiments. The resultant plots can be found in the Supporting Information. Using this method, the loading of the samples from the WWC could be obtained, which in turn allowed the speciation of the WWC samples to be determined from the NMR results of the standard solutions.

The UV−vis spectra were analyzed at three different levels of transmission (75, 50, and 25%) so that the loading of the samples could be determined unambiguously (giving three independent data points instead of one), particularly at higher loadings and higher vanadium concentrations where the UV−vis spectra were less sensitive to changes in loading. Ideally it would have been better to use the peak location, instead of the transmission shoulder, but this was not possible as the vanadate species strongly absorbed light in the region 350−400 nm, and the samples could not be diluted due to it changing the vanadate speciation (and thus UV−vis absorption).

Wetted Wall Column Experiments. The observed rate constant for the absorption of CO_2 in 30% w/w K_2CO_3 as a function of concentration of $K_4V_2O_7$ at 40, 60, and 75 °C is given in Figure 5a. The solutions were typically preloaded with $KHCO_3$ to an equivalent loading of 0.15 to ensure steady CO_2 absorption was achieved within a reasonable time frame. At this time the CO_2 absorption could be assumed to be under pseudo-steady-state conditions. Under these conditions the absorption of CO_2 does not significantly affect the pH of the system.

Furthermore, at 60 °C a second set of experiments were run at 0.05 initial loading to determine if initial loading (and subsequent changes in speciation) affected the rate of CO_2 absorption. A summary of the experimental parameters used to determine the observed rate constant for each experiment can be found in the Supporting Information.

Once the contributions from water (which was negligible in this work) and hydroxide ions were removed from the observed rate constant (Figure 5b), it was found that the reduced first-order rate constant, k'_{obs}, has a nonzero value. This indicates that the absorption rate of CO_2 is increased by the presence of vanadium. Also, given that at 60 °C the 0.05 and 0.15 initially loaded solutions showed no discernible difference in CO_2 absorption rate, it is concluded that loading has a lesser effect

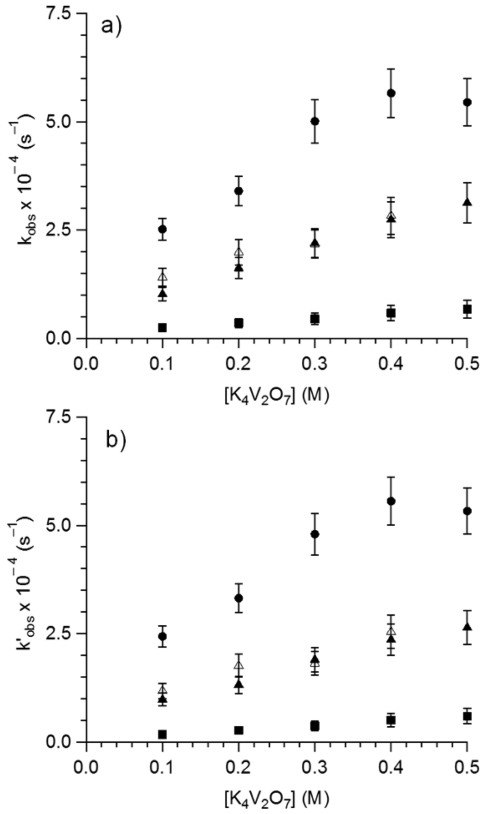

Figure 5. (a) Observed rate constant for CO_2 hydration in 30% w/w K_2CO_3 with different $K_4V_2O_7$ concentrations. (b) Observed rate constant with contributions from the reaction with water and hydroxide subtracted. (■) 40 °C, 0.15 initial loading; (▲) 60 °C, 0.15 initial loading; (△) 60 °C, 0.05 initial loading; (●) 75 °C, 0.15 initial loading.

on the absorbance of CO_2 compared to the concentration of $K_4V_2O_7$ added.

While the results show that the presence of vanadium enhances the rate of CO_2 absorption, it is not clear which of the vanadate ions are responsible for this increase. To determine this, k'_{obs} was plotted vs the concentration of each vanadate ion for a given temperature (Figure 6). It was observed that k'_{obs} was typically linearly dependent upon each species (with the exception of HVO_4^{2-}, where no dependence was observed) but with a nonzero observed rate constant at zero concentration. This indicates that there is more than one active species of vanadium present.

To isolate which species are acting as promoters, a fitted reduced first-order rate constant, k'_{calc}, was expressed as contributions from each species present (except the central vanadate ions of trimer/tetramer species, for reasons explained later), each with their own reaction rate constant k_i as shown by eq 12:

$$k'_{calc} = k_{HVO_4}[HVO_4^{2-}] + k_{V_2O_7}[V_2O_7^{4-}] + k_{HV_2O_7}[HV_2O_7^{3-}] + k_{V\text{-}CO_2}[V\text{-}CO_2] + k_{V_3/V_4}[V_3O_{10}^{5-} + V_4O_{13}^{6-}] \quad (12)$$

k'_{calc} vs k'_{obs} was then plotted, with the k_i for each vanadate species as fitted parameters (subjected to the constraint that they must be a positive value), so that the resultant plot was a straight line with a gradient of 1 and an intercept of 0. The

dx.doi.org/10.1021/ie403836e | Ind. Eng. Chem. Res. 2014, 53, 3029−3039

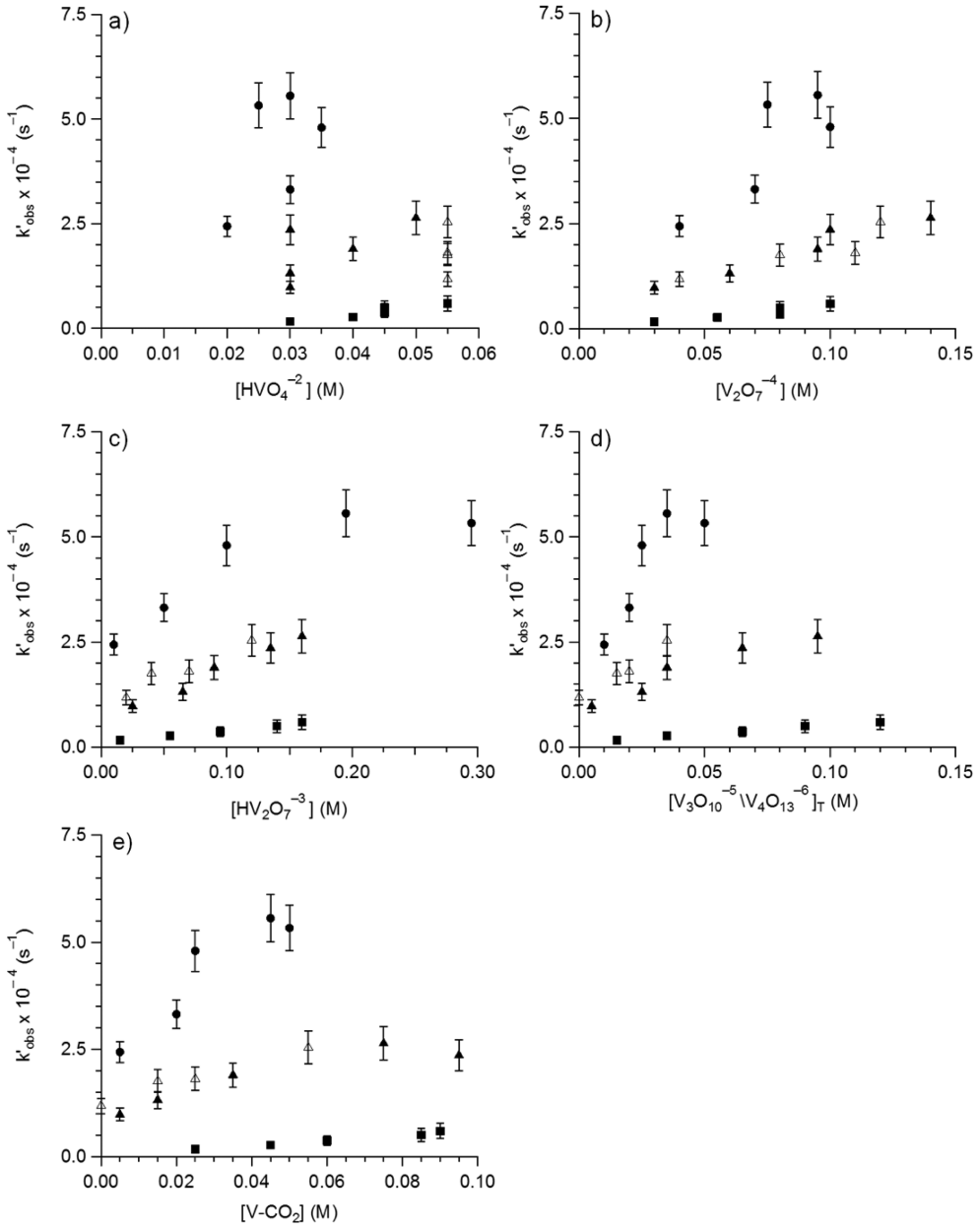

Figure 6. Reduced rate constant for CO_2 hydration in 30% w/w K_2CO_3 plotted against concentrations of each vanadate ion observed. (a) HVO_4^{2-}, (b) $V_2O_7^{4-}$, (c) $HV_2O_7^{3-}$, (d) terminal vanadates of $V_3O_{10}^{5-}/V_4O_{13}^{6-}$, and (e) vanadate carbonate complex. (■) 40 °C, 0.15 initial loading; (▲) 60 °C, 0.15 initial loading; (△) 60 °C, 0.05 initial loading; (●) 75 °C, 0.15 initial loading.

determined values of k_i then represent the reaction rate constants for each vanadate species. The number of fitted parameters was then systematically reduced to determine which were the key parameters of the fit. The k_i for one component was then set to 0 (such that there were now only four active species) and the remaining k_i values were readjusted as before. This process was repeated, each time excluding a different species of vanadium, and then repeated for three and two active species, thus testing every possible combination of active species. It was found, however, that only specific combinations of vanadium species were able to provide a zero intercept while maintaining positive k_i values. Thus, using this analysis method, it was determined that HVO_4^{2-}, $HV_2O_7^{3-}$, and the CO_2 complex were all potentially active species. However, when all three components were together, the CO_2 complex had a comparatively lower rate constant than HVO_4^{2-} and $HV_2O_7^{3-}$. Furthermore, as the CO_2 complex is a product of the reaction between CO_2 and vanadium, it is expected that it should increase with an increasing rate of CO_2 absorption. Therefore, the CO_2 complex was discounted as being an active species, meaning that HVO_4^{2-} and $HV_2O_7^{3-}$ are the reactive species in CO_2 absorption, and the rate constants reported in this work are the result of the two parameter fit using HVO_4^{2-} and $HV_2O_7^{3-}$.

That these vanadium species catalyze the hydration of CO_2 is supported by the work of Sharma and Danckwerts,[36] as they suggested that the presence of both −OH and $-O^-$ groups attached to a central atom were a key element for the catalysis of CO_2 hydration. This also supports the choice to set the reaction order as 1 for all species as it has been previously observed that these types of molecules are typically involved in first-order reactions (with respect to the promoter) with CO_2.

dx.doi.org/10.1021/ie403836e | *Ind. Eng. Chem. Res.* 2014, 53, 3029−3039

Table 2. Reaction Rate Constants of the Active Species in $K_4V_2O_7/K_2CO_3$ Solutions under the Different Conditions Studied

temp (°C)	init loading	k_{HVO_4} (M^{-1} s^{-1})	$k_{HV_2O_7}$ (M^{-1} s^{-1})	k_{OH}[a] (M^{-1} s^{-1})
40	0.15	$(3.9 \pm 0.9) \times 10^4$	$(2.3 \pm 0.5) \times 10^4$	2.66×10^5
60	0.15	$(2.6 \pm 0.7) \times 10^5$	$(8.4 \pm 2.3) \times 10^4$	6.07×10^5
60	0.05	$(2.6 \pm 1.2) \times 10^5$	$(9.7 \pm 2.7) \times 10^4$	6.07×10^5
75	0.15	$(1.20 \pm 0.2) \times 10^6$	$(1.04 \pm 0.2) \times 10^5$	1.06×10^6

[a] k_{OH} was calculated from previously determined values.[27]

Therefore, by fitting the concentrations of HVO_4^{2-} and $HV_2O_7^{3-}$ against the observed rate constant at different $K_4V_2O_7$ concentrations and different temperatures, the reaction rate constants for these two species could be determined. Table 2 shows the resultant rate constants for HVO_4^{2-} and $HV_2O_7^{3-}$ obtained from this work, as well as the rate constant for OH^-.

Using the rate constants in Table 2 and the concentrations of HVO_4^{2-}, $HV_2O_7^{3-}$, and OH^-, the contributions of each reaction could be determined as a function of total vanadium concentration at different temperatures, the results of which are shown in Figure 7. From Figure 7 it can be seen that as the total vanadium concentration increases the contribution from hydroxide ions decreases, while the contribution from HVO_4^{2-} goes through a maximum at low (<0.1 M $K_4V_2O_7$) concentrations and the contribution from $HV_2O_7^{3-}$ tends to increase. This is due to the relative changes in HVO_4^{2-} and $HV_2O_7^{3-}$ concentrations as the total vanadium concentration increases. This explains the plateau in the observed rate constant (Figure 5a) at high $K_4V_2O_7$ concentrations as the faster reaction with HVO_4^{2-} declines and the slower reaction with $HV_2O_7^{3-}$ becomes the dominating reaction.

The activation energy of the reaction between each species and CO_2 can be determined by fitting an Arrhenius function to the rate constant data as a function temperature. Plots of $\ln(k_i)$ vs $1/T$ are given in Figure 8. From these plots the activation energy can be obtained from the gradient of each plot and the pre-exponential factor from the intercept. From the data in Figure 8 the following expressions were determined for the temperature dependence of HVO_4^{2-} and $HV_2O_7^{3-}$:

$$k_{HVO_4} = 2 \times 10^{11} e^{-4992/T} \quad (13)$$

$$k_{HV_2O_7} = 5 \times 10^{18} e^{-10218/T} \quad (14)$$

which gives activation energies for reactions between CO_2 and HVO_4^{2-} and between CO_2 and $HV_2O_7^{3-}$ of 41.5 and 85.0 kJ/mol, respectively.

The primary source of error in this work was measuring the gas flow out of the wetted wall column as it was observed to fluctuate by ca. ±30 mL/min during the course of an experiment. The standard deviations of the corresponding minimum, maximum, and observed values resulting from this error range were propagated throughout the analysis to give an indication of the maximum error range in the values reported in this paper.

The central vanadate atoms in the trimer/tetramer ions were not considered in the reaction with CO_2 for several reasons. First, they are not known to be as reactive as the terminal vanadate anions, and second, it was observed that another unidentified vanadium species was also present in the −554 to −556 ppm range. This was evident by the fact that the terminal to central vanadate ratio was often not between 1 (indicating solely tetramer present) and 2 (indicating solely trimer). Furthermore, a peak in that location was observed with no corresponding peak in the terminal range. It was suspected that this peak could be due to the carbonated metavanate ($VO_2 \cdot CO_2$), but this was discounted as it has previously been shown that metavanadate and carboxylic acids exchange more rapidly

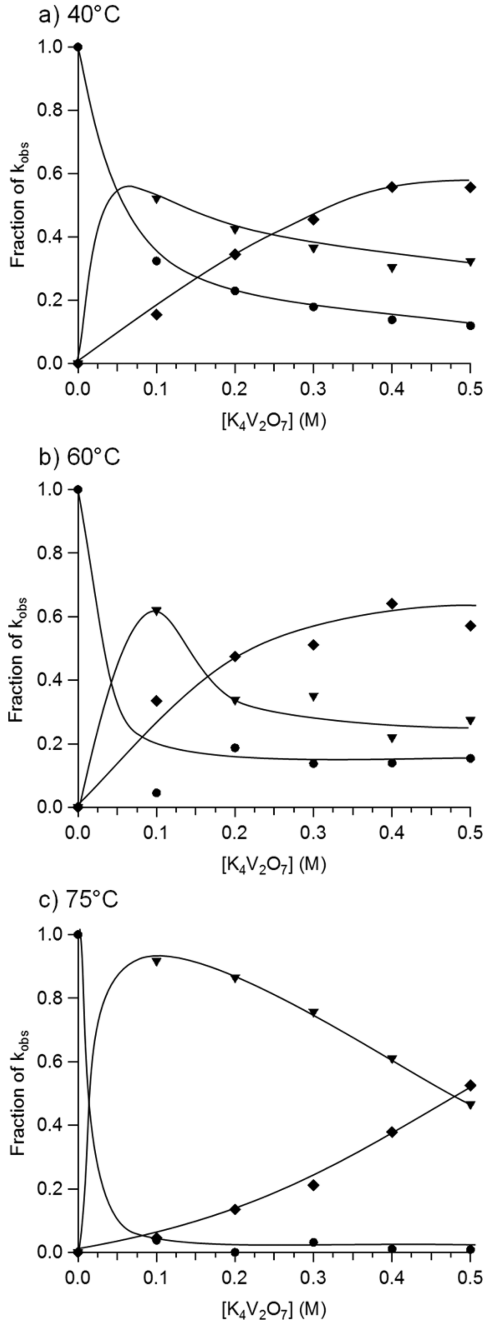

Figure 7. Contribution of OH^- (●), HVO_4^{2-} (▼), and $HV_2O_7^{3-}$ (◆) to observed rate constant for CO_2 hydration in 30% w/w K_2CO_3 at (a) 40, (b) 60, and (c) 75 °C. Lines added as a guide to the eye.

dx.doi.org/10.1021/ie403836e | Ind. Eng. Chem. Res. 2014, 53, 3029−3039

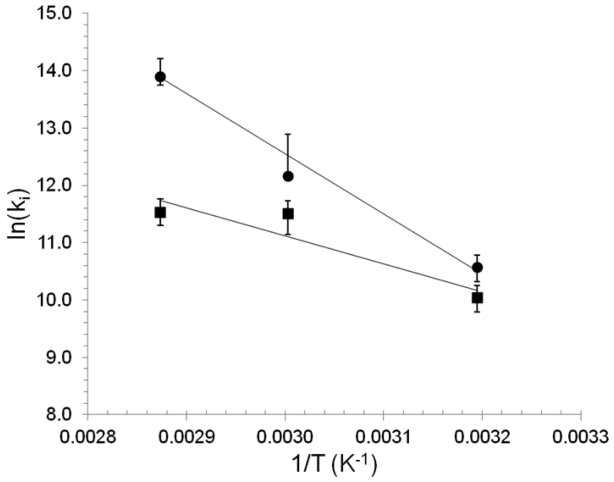

Figure 8. Arrhenius plots of reaction rate constants for HVO_4^{2-} (●) and $HV_2O_7^{3-}$ (■) with CO_2 in 30% w/w K_2CO_3.

than the time scale of an NMR measurement.[53] This causes the two species to appear as a single, broader peak between the two peak values (carbonated and noncarbonated), which was what was observed in this work.

Comparison with Other Promoters. Table 3 compares the reaction rate constants between CO_2 and several other inorganic promoters, with MEA and piperazine added for comparison. From Table 3 it is apparent that both active vanadate species react with CO_2 at a much faster rate than other inorganic species that have been previously studied, by at least an order of magnitude. Furthermore, it can be seen that the reaction rates are comparable and indeed exceed that of MEA but are still about an order of magnitude below that of piperazine. However, due to the speciation behavior of aqueous vanadium ions (i.e., as vanadium concentration increases, the relative concentrations of active species tend to decrease), the overall performance of vanadium as a promoter for CO_2 capture is less than that of MEA, as the concentration of active MEA can be on the order of 1−15 M, as opposed to 0.05 or 0.30 M for HVO_4^{2-} and $HV_2O_7^{3-}$.

This limitation in active species of aqueous vanadium solutions indicates that it would be more suitable as a secondary promoter in a potassium carbonate solution, offering further enhancement to an already promoted system. Not only would the presence of a small amount of vanadium enhance the rate of CO_2 absorption, it can also act as a corrosion inhibitor, and previous studies[33] have shown that the addition of as little as 100 ppm (ca. 5 mM) vanadium can reduce the corrosivity of amine solutions by at least 3 orders of magnitude. Using lower concentrations of vanadium will also limit the potentially adverse environmental effects associated with vanadate solutions (which are often considered toxic).

Table 3. Reaction Rate Constants for Different Inorganic Promoters

promoter	temp (°C)	solution	k_i (s^{-1})	exptl method	ref
$B(OH)_4^-$	40	2.8 M K_2CO_3	148	wetted wall column	27
$HAsO_3^{2-}$	25	0.33 M K_2CO_3	164	wetted wall column	37
$HAsO_3^{2-}$	40	1.5 M K_2CO_3	1 460	liquid jet	39
ClO^-	35	0.5 M Na_2CO_3	3 040	liquid jet	39
HVO_4^{2-}	40	2.8 M K_2CO_3	38 800	wetted wall column	this work
$HV_2O_7^{3-}$	40	2.8 M K_2CO_3	22 900	wetted wall column	this work
MEA	40	2.8 M K_2CO_3	20 900	wetted wall column	29
piperazine	25	1.81 M $KHCO_3$	236 000[a]	wetted wall column	28

[a]Estimated using a pseudo-first-order analysis.

CONCLUSIONS

The kinetics of absorption of CO_2 in vanadium promoted carbonate solutions, as well as the speciation profiles of the vanadium anions, has been presented in this work. It was found that the addition of vanadium significantly increased the overall rate of CO_2 absorption by reaction with two vanadium species, HVO_4^{2-} and $HV_2O_7^{3-}$, both of which have rate constants comparable to that of MEA. However, the speciation of vanadium is heavily dependent upon vanadium concentration, with HVO_4^{2-} (the more reactive species) becoming less prevalent at higher total vanadium concentrations. This limits the effectiveness of vanadium(V) as it remains in small concentrations. However, vanadium may still be useful, providing additional enhancement in carbonate solutions containing another primary promoter.

ASSOCIATED CONTENT

Supporting Information

A list of experimental values used in this work, speciation diagrams for the different vanadate ions in 30% w/w K_2CO_3 as a function of $K_4V_2O_7$ concentration, CO_2 loading and temperature, as well as the UV−vis standard graphs used to determine the CO_2 loading of the solution. This material is available free of charge via the Internet at http://pubs.acs.org.

AUTHOR INFORMATION

Corresponding Author

*E-mail: gstevens@unimelb.edu.au.

Notes

The authors declare no competing financial interest.

ACKNOWLEDGMENTS

The authors of this work acknowledge support for this CO2CRC research project provided by the Australian government through its CRC program as well as support from the Particulate Fluids Processing Centre (PFPC) at the University of Melbourne.

REFERENCES

(1) Summary for Policymakers. In *Climate Change 2007: The Physical Science Basis. Contribution of Working Group I to the Fourth Assessment Report of the Intergovernmental Panel on Climate Change*; Solomon, S., Qin, D., Manning, M., Chen, Z., Marquis, M., Averyt, K. B., Tignor, M., Miller, H. L., Eds.; Cambridge University Press: Cambridge, U.K., 2007; 18 pp.

(2) Petit, J. R.; Jouzel, J.; Raynaud, D.; Barkov, N. I.; Barnola, J. M.; Basile, I.; Bender, M.; Chappellaz, J.; Davis, M.; Delaygue, G.; Delmotte, M.; Kotlyakov, V. M.; Legrand, M.; Lipenkov, V. Y.; Lorius, C.; Pepin, L.; Ritz, C.; Saltzman, E.; Stievenard, M. Climate and Atmospheric History of the Past 420,000 Years from the Vostok Ice Core, Antarctica. *Nature* **1999**, *399* (6735), 429−436.

(3) Parmesan, C.; Yohe, G. A Globally Coherent Fingerprint of Climate Change Impacts across Natural Systems. *Nature* **2003**, *421* (6918), 37−42.
(4) Siegenthaler, U.; Sarmiento, J. L. Atmospheric Carbon-Dioxide and the Ocean. *Nature* **1993**, *365* (6442), 119−125.
(5) Caldeira, K.; Wickett, M. E. Anthropogenic Carbon and Ocean pH. *Nature* **2003**, *425* (6956), 365−365.
(6) Orr, J. C.; Fabry, V. J.; Aumont, O.; Bopp, L.; Doney, S. C.; Feely, R. A.; Gnanadesikan, A.; Gruber, N.; Ishida, A.; Joos, F.; Key, R. M.; Lindsay, K.; Maier-Reimer, E.; Matear, R.; Monfray, P.; Mouchet, A.; Najjar, R. G.; Plattner, G. K.; Rodgers, K. B.; Sabine, C. L.; Sarmiento, J. L.; Schlitzer, R.; Slater, R. D.; Totterdell, I. J.; Weirig, M. F.; Yamanaka, Y.; Yool, A. Anthropogenic Ocean Acidification over the Twenty-First Century and Its Impact on Calcifying Organisms. *Nature* **2005**, *437* (7059), 681−686.
(7) Doney, S. C.; Fabry, V. J.; Feely, R. A.; Kleypas, J. A. Ocean Acidification: The Other CO2 Problem. In *Annual Review of Marine Science*; Annual Reviews: Palo Alto, CA, 2009; Vol. *1*, pp 169−192.
(8) Aaron, D.; Tsouris, C. Separation of CO2 from Flue Gas: A Review. *Sep. Sci. Technol.* **2005**, *40* (1−3), 321−348.
(9) Yang, H. Q.; Xu, Z. H.; Fan, M. H.; Gupta, R.; Slimane, R. B.; Bland, A. E.; Wright, I. Progress in Carbon Dioxide Separation and Capture: A Review. *J. Environ. Sci.* **2008**, *20* (1), 14−27.
(10) Bishnoi, S.; Rochelle, G. T. Absorption of Carbon Dioxide into Aqueous Piperazine: Reaction Kinetics, Mass Transfer and Solubility. *Chem. Eng. Sci.* **2000**, *55* (22), 5531−5543.
(11) Dugas, R. E.; Rochelle, G. T. CO2 Absorption Rate into Concentrated Aqueous Monoethanolamine and Piperazine. *J. Chem. Eng. Data* **2011**, *56* (5), 2187−2195.
(12) Horng, S.-Y.; Li, M.-H. Kinetics of Absorption of Carbon Dioxide into Aqueous Solutions of Monoethanolamine and Triethanolamine. *Ind. Eng. Chem. Res.* **2002**, *41* (2), 257−266.
(13) Astarita, G. Carbon Dioxide Absorption in Aqueous Monoethanolamine Solutions. *Chem. Eng. Sci.* **1961**, *16* (3−4), 202−207.
(14) Clarke, J. K. A. Kinetics of Absorption of Carbon Dioxide in Monoethanolamine Solutions at Short Contact Times. *Ind. Eng. Chem. Fundam.* **1964**, *3* (3), 239−245.
(15) Jou, F.-Y.; Mather, A. E.; Otto, F. D. The Solubility of CO2 in a 30 Mass Percent Monoethanolamine Solution. *Can. J. Chem. Eng.* **1995**, *73* (1), 140−147.
(16) Martin, S.; Lepaumier, H.; Picq, D.; Kittel, J.; de Bruin, T.; Faraj, A.; Carrette, P.-L. New Amines for CO2 Capture. IV. Degradation, Corrosion, and Quantitative Structure Property Relationship Model. *Ind. Eng. Chem. Res.* **2012**, *51* (18), 6283−6289.
(17) Nguyen, T.; Hilliard, M.; Rochelle, G. T. Amine Volatility in CO_2 Capture. *Int. J. Greenhouse Gas Control* **2010**, *4* (5), 707−715.
(18) Goff, G. S.; Rochelle, G. T. Monoethanolamine Degradation: O_2 Mass Transfer Effects under CO_2 Capture Conditions. *Ind. Eng. Chem. Res.* **2004**, *43* (20), 6400−6408.
(19) Strazisar, B. R.; Anderson, R. R.; White, C. M. Degradation Pathways for Monoethanolamine in a CO_2 Capture Facility. *Energy Fuels* **2003**, *17* (4), 1034−1039.
(20) Supap, T.; Idem, R.; Tontiwachwuthikul, P.; Saiwan, C. Analysis of Monoethanolamine and Its Oxidative Degradation Products During CO_2 Absorption from Flue Gases: A Comparative Study of GC-MS, HPLC-RID, and CE-DAD Analytical Techniques and Possible Optimum Combinations. *Ind. Eng. Chem. Res.* **2005**, *45* (8), 2437−2451.
(21) Supap, T.; Idem, R.; Tontiwachwuthikul, P.; Saiwan, C. Kinetics of Sulfur Dioxide- and Oxygen-Induced Degradation of Aqueous Monoethanolamine Solution During CO2 Absorption from Power Plant Flue Gas Streams. *Int. J. Greenhouse Gas Control* **2009**, *3* (2), 133−142.
(22) Buck, B. O.; Leitch, A. R. S. Try Gas Treating with Hot Carbonate. *Pet. Refin.* **1958**, *37*, 241−246.
(23) Benson, H. E.; Field, J. H.; Jimeson, R. M. CO_2 Absorption: Employing Hot Potassium Carbonate Solutions. *Chem. Eng. Prog.* **1954**, *50* (7), 356−364.
(24) Benson, H. E.; Field, J. H.; Haynes, W. P. Improved Process for Carbon Dioxide Absorption Uses Hot Carbonate Solutions. *Chem. Eng. Prog.* **1956**, *52* (10), 433−438.
(25) Mumford, K. A.; Smith, K. H.; Anderson, C. J.; Shen, S.; Tao, W.; Suryaputradinata, Y. A.; Qader, A.; Hooper, B.; Innocenzi, R. A.; Kentish, S. E.; Stevens, G. W. Post-Combustion Capture of CO2: Results from the Solvent Absorption Capture Plant at Hazelwood Power Station Using Potassium Carbonate Solvent. *Energy Fuels* **2011**, *26* (1), 138−146.
(26) Knuutila, H.; Juliussen, O.; Svendsen, H. F. Kinetics of the Reaction of Carbon Dioxide with Aqueous Sodium and Potassium Carbonate Solutions. *Chem. Eng. Sci.* **2010**, *65* (23), 6077−6088.
(27) Thee, H.; Smith, K. H.; da Silva, G.; Kentish, S. E.; Stevens, G. W. Carbon Dioxide Absorption into Unpromoted and Borate-Catalyzed Potassium Carbonate Solutions. *Chem. Eng. J.* **2012**, *181−182*, 694−701.
(28) Cullinane, J. T.; Rochelle, G. T. Kinetics of Carbon Dioxide Absorption into Aqueous Potassium Carbonate and Piperzine. *Ind. Eng. Chem. Res.* **2006**, *45* (8), 2531−2545.
(29) Thee, H.; Suryaputradinata, Y. A.; Mumford, K. A.; Smith, K. H.; da Silva, G.; Kentish, S. E.; Stevens, G. W. A Kinetic and Process Modeling Study of CO2 Capture with MEA-Promoted Potassium Carbonate Solutions. *Chem. Eng. J.* **2012**, *210*, 271−279.
(30) Guo, D.; Thee, H.; Tan, C. Y.; Chen, J.; Fei, W.; Kentish, S.; Stevens, G. W.; da Silva, G. Amino Acids as Carbon Capture Solvents: Chemical Kinetics and Mechanism of the Glycine + CO_2 Reaction. *Energy Fuels* **2013**, *27* (7), 3898−3904.
(31) Kumar, P. S.; Hogendoorn, J. A.; Versteeg, G. F.; Feron, P. H. M. Kinetics of the Reaction of CO_2 with Aqueous Potassium Salt of Taurine and Glycine. *AIChE J.* **2003**, *49* (1), 203−213.
(32) Portugal, A. F.; Sousa, J. M.; Magalhães, F. D.; Mendes, A. Solubility of Carbon Dioxide in Aqueous Solutions of Amino Acid Salts. *Chem. Eng. Sci.* **2009**, *64* (9), 1993−2002.
(33) Ahn, S.; Song, H.-J.; Park, J.-W.; Lee, J. H.; Lee, I. Y.; Jang, K.-R. Characterization of Metal Corrosion by Aqueous Amino Acid Salts for the Capture of CO_2. *Korean J. Chem. Eng.* **2010**, *27* (5), 1576−1580.
(34) McCann, N.; Phan, D.; Wang, X.; Conway, W.; Burns, R.; Attalla, M.; Puxty, G.; Maeder, M. Kinetics and Mechanism of Carbamate Formation from CO2(aq), Carbonate Species, and Monoethanolamine in Aqueous Solution. *J. Phys. Chem. A* **2009**, *113* (17), 5022−5029.
(35) Guo, D.; Thee, H.; da Silva, G.; Chen, J.; Fei, W.; Kentish, S.; Stevens, G. W. Borate-Catalyzed Carbon Dioxide Hydration Via the Carbonic Anhydrase Mechanism. *Environ. Sci. Technol.* **2011**, *45* (11), 4802−4807.
(36) Sharma, M. M.; Danckwerts, P. V. Catalysis by Bronsted Bases of the Reaction between CO_2 and Water. *Trans. Faraday Soc.* **1963**, *59*, 386−395.
(37) Roberts, D.; Danckwerts, P. V. Kinetics of CO_2 Absorption in Alkaline Solutions. 1. Transient Absorption Rates and Catalysis by Arsenite. *Chem. Eng. Sci.* **1962**, *17* (12), 961−969.
(38) Kumar, N.; Rao, D. P. Design of a Packed Column for Absorption of Carbon Dioxide in Hot K2CO3 Solution Promoted by Arsenious Acid. *Gas Sep. Purif.* **1989**, *3* (3), 152−155.
(39) Sharma, M. M.; Danckwerts, P. V. Fast Reactions of CO_2 in Alkaline Solutions. A. Carbonate Buffers with Arsenite, Formaldehyde and Hypochlorite as Catalysts. B. Aqueous Monoisopropanolamine (1-Amino-2-Propanol) Solutions. *Chem. Eng. Sci.* **1963**, *18* (12), 729−735.
(40) Le, Q.; Tu, J.; Shi, Y. Catalytic Activity of Vanadium Pentoxide for the Absorption of Carbon Dioxide by Potassium Carbonate Solution. *Acta Phys.-Chim. Sin.* **1992**, *8* (6), 753−759.
(41) Khalifah, R. G. Carbon Dioxide Hydration Activity of Carbonic Anhydrase. 1. Stop-Flow Kinetic Studies on Native Human Isoenzyme-B and Isoenzyme-C. *J. Biol. Chem.* **1971**, *246* (8), 2561.
(42) Crans, D. C.; Tracey, A. S. The Chemistry of Vanadium in Aqueous and Nonaqueous Solution. In *Vanadium Compounds: Chemistry, Biochemistry, and Therapeutic Applications*; ACS Symposium

Series 711; American Chemical Society: Washington, DC, 1998; pp 2−29.
(43) Howarth, O. W.; Richards, R. E. Nuclear Magnetic Resonance Study of Polyvanadate Equilibria by Use of Vanadium-51. *J. Chem. Soc.* **1965**, No. Feb, 864.
(44) Vermaire, S.; De Haan, R. Influence of Sodium-Carbonate Vanadium Concentration Ratios on Vanadate(V) Equilibria and on the Reoxidation of V(IV) in a Hydrogen Sulfide Removal Process. *Ind. Eng. Chem. Res.* **1988**, *27* (7), 1242−1245.
(45) Tseng, P. C.; Ho, W. S.; Savage, D. W. Carbon Dioxide Absorption into Promoted Carbonate Solutions. *AIChE J.* **1988**, *34* (6), 922−931.
(46) Ratcliff, G. A.; Holdcroft, J. G. Diffusivities of Gases in Aqueous Electrolyte Solutions. *Trans. Inst. Chem. Eng.* **1963**, *41* (10), 315−319.
(47) Versteeg, G. F.; Blauwhoff, P. M. M.; Van Swaaij, W. P. M. The Effect of Diffusivity on Gas-Liquid Mass Transfer in Stirred Vessels. Experiments at Atmospheric and Elevated Pressures. *Chem. Eng. Sci.* **1987**, *42* (5), 1103−1119.
(48) Joosten, G. E. H.; Danckwerts, P. V. Solubility and Diffusivity of Nitrous Oxide in Equimolar Potassium Carbonate-Potassium Bicarbonate Solutions at 25°C and 1 atm. *J. Chem. Eng. Data* **1972**, *17* (4), 452−454.
(49) Kumar, P. S.; Hogendoorn, J. A.; Feron, P. H. M.; Versteeg, G. F. Density, Viscosity, Solubility, and Diffusivity of N2O in Aqueous Amino Acid Salt Solutions. *J. Chem. Eng. Data* **2001**, *46* (6), 1357−1361.
(50) Knuutila, H.; Juliussen, O.; Svendsen, H. F. Density and N2O Solubility of Sodium and Potassium Carbonate Solutions in the Temperature Range 25 to 80 °C. *Chem. Eng. Sci.* **2010**, *65* (6), 2177−2182.
(51) Heath, E.; Howarth, O. W. V-51 and O-17 Nuclear Magnetic-Resonance Study of Vanadate (V) Equilibria and Kinetics. *J. Chem. Soc., Dalton Trans.* **1981**, *5*, 1105−1110.
(52) Cruywagen, J. J.; Heyns, J. B. B.; Westra, A. N. Vanadium(V) Equilibria: Thermodynamic Quantities for Some Protonation and Condensation Reactions. In *Vanadium Compounds: Chemistry, Biochemistry, and Therapeutic Applications*; ACS Symposium Series 711; American Chemical Society: Washington, DC, 1998; pp 51−59.
(53) Tracey, A. S.; Li, H. L.; Gresser, M. J. Interactions of Vanadate with Monocarboxylic and Dicarboxylic-Acids. *Inorg. Chem.* **1990**, *29* (12), 2267−2271.